Reductive Dimerization of $[Mo(C_6F_5)(CO)_2(\eta\text{-}C_7H_7)]$. Synthesis and Characterization of the Bitropyl Complex $[\{Mo(C_6F_5)(CO)_2\}_2(\eta^6:\eta'^6\text{-}C_{14}H_{14})]^{2-}$ †

Mingzhong Su, Stephen L. Gipson,* Donald F. Mullica,* Eric L. Sappenfield and Dale Hugo Leschnitzer

Department of Chemistry, Baylor University, Waco, TX 76798, USA

The complex $[Mo(C_6F_5)(CO)_2(\eta\text{-}C_7H_7)]$ **1** can be reduced either chemically or electrochemically (E_{pc} = −2.07 V *vs.* ferrocenium–ferrocene) by one electron to produce the bitropyl (bicycloheptatrienyl) complex $[\{Mo(C_6F_5)(CO)_2\}_2(\eta^6:\eta'^6\text{-}C_{14}H_{14})]^{2-}$ $\mathbf{2}^{2-}$. The sodium salt produced by Na(Hg) reduction of **1** in tetrahydrofuran is extremely air sensitive, but replacement of the Na^+ cations with $[N(PPh_3)_2]^+$ yields a much more stable salt. With either counter ion, the complex $\mathbf{2}^{2-}$ exists in solution as a mixture of three isomers: *endo-endo*; *endo-exo*; and *exo-exo*. The complex has been fully characterized by IR, ^1H and ^{13}C NMR spectroscopy, elemental analysis and a crystal structure of the *endo-endo* isomer of the $[N(PPh_3)_2]^+$ salt. Oxidation of the bitropyl complex rapidly cleaves the bridging C–C bond and returns complex **1**.

We have been been investigating the electrochemistry and redox reactivity of $[Mo(C_6F_5)(CO)_2(\eta\text{-}C_7H_7)]$ **1**, one of the few stable cycloheptatrienyl (tropyl) analogues of the large family of cyclopentadienylmolybdenum alkyl and aryl carbon complexes. In dichloromethane compound **1** displays a reversible one-electron oxidation at +0.49 V *vs.* ferrocenium–ferrocene.[1] The one-electron reduction of **1** (E_{pc} = −2.07 V) is followed by a reversible structural change producing a previously unidentified orange product. Reaction of this product with trimethyl phosphite in tetrahydrofuran (thf) yields the pale yellow complex Na[*cis-mer*-$Mo(C_6F_5)(CO)_2\{P(OMe)_3\}_3$].[2]

The reductions of the cationic tricarbonyl complexes $[M(CO)_3(\eta\text{-}C_7H_7)]^+$ (M = Cr, Mo or W) have been studied extensively.[3] These complexes undergo initial two-electron reductions,[4] followed by coupling of the resulting anions with the cationic starting materials to yield neutral $\eta^6:\eta'^6$-bitropyl complexes. Dimetal bitropyl complexes have been shown to exist as three isomers,[3d] labelled according to the orientation of the hydrogen atoms attached to the bridging carbon atoms of the bitropyl ligand. Since these hydrogens may be either *endo* or *exo* with respect to the metal atom complexed to each half of the bitropyl ligand, the complexes may exist as *endo-endo*, *endo-exo* and *exo-exo* isomers.

We now report that the product of the reduction of **1** is a bitropyl complex, $[\{Mo(C_6F_5)(CO)_2\}_2(\eta^6:\eta'^6\text{-}C_{14}H_{14})]^{2-}$ $\mathbf{2}^{2-}$. It was not previously possible to isolate this species because of the air sensitivity of its sodium salt. It has now been fully characterized by IR, ^1H and ^{13}C NMR spectroscopy, elemental analysis and the crystal structure of the *endo-endo* isomer of the $[N(PPh_3)_2]^+$ salt.

Results and Discussion

Electrochemistry of $[Mo(C_6F_5)(CO)_2(\eta\text{-}C_7H_7)]$ **1** *in thf.*—Cyclic voltammetry of complex **1** in thf displays a reversible one-electron oxidation at +0.49 V *vs.* ferrocenium–ferrocene and an apparently irreversible reduction with a cathodic peak potential of −2.07 V coupled to a smaller anodic peak at −0.86 V [Fig. 1(*a*)]. Controlled-potential electrolysis of a green 2 mmol dm^{-3} solution of **1** at −2.20 V *vs.* ferrocenium–ferrocene in thf consumed 0.98 F per mol and produced a dark orange solution of a product which we will here label $\mathbf{2}^{2-}$ (*cf.* $\mathbf{1}^-$ in ref. 2). Cyclic voltammetry after the electrolysis showed an anodic peak at −0.83 V coupled to a smaller cathodic peak at −2.01 V

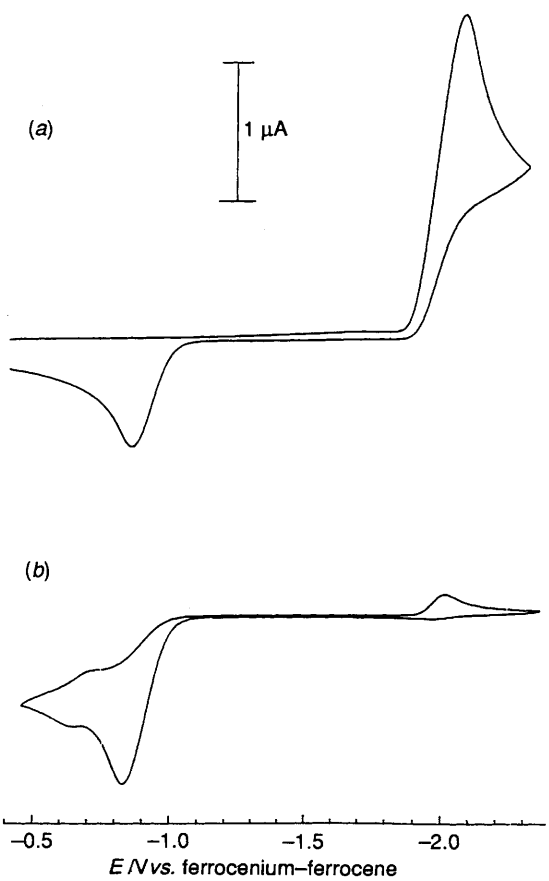

Fig. 1 Cyclic voltammograms of $[Mo(C_6F_5)(CO)_2(\eta\text{-}C_7H_7)]$ **1** in thf (*a*) initial and (*b*) after electrolysis at −2.20 V

† *Supplementary data available:* see Instructions for Authors, *J. Chem. Soc., Dalton Trans.*, 1993, Issue 1, pp. xxiii–xxviii.

[Fig. 1(*b*)]. Fig. 1(*b*) also shows a small reversible couple with a formal potential of −0.69 V. This couple was not observed in all experiments and most likely originates from a decomposition product of 2^{2-}, probably similar to the tris(trimethyl phosphite) complex previously reported.[2] Species 2^{2-} can be reoxidized at −0.35 V, requiring approximately 2 F per mol and returning the green colour and cyclic voltammogram of **1**.[2] Since the cathodic peak current after reoxidation is the same as that before controlled-potential reduction, regeneration of **1** is judged to be quantitative.

Having established that complex 2^{2-} results from the reductive dimerization of **1** (see below), we were curious as to which of the several possible mechanisms might be involved. Dimerization might result from radical–radical coupling of 1^- (DIM1), radical–substrate coupling (DISP1 or DISP2), or ion–substrate coupling (DIM3).[5] Romanin *et al.*[4a] established that the reductive dimerization of $[Cr(CO)_3(\eta\text{-}C_7H_7)]^+$ proceeds by the DIM3 mechanism. However, for compound **1** the slopes of plots of peak potential *vs.* log v from linear-sweep voltammetry were 19–20 mV per decade. This result is consistent with the DIM1 and DISP1/DISP2 mechanisms, but not DIM3.[5] The net effect of either possible mechanism is a radical–radical coupling, and so we are inclined to describe the reductive dimerization of **1** as a one-electron reduction followed by coupling of the resulting 1^- radical anions. The rate of the dimerization must be very large since no anodic peak corresponding to the reoxidation of 1^- could be observed by cyclic voltammetry at scan rates of up to 200 V s^{-1}.

Synthesis and Characterization of the Na^+ *and* $[N(PPh_3)_2]^+$ *Salts of* 2^{2-}.—As has been reported previously,[2] compound **1** may be reduced by Na(Hg) in thf to produce the orange salt of 2^{2-}. However, all attempts to isolate and purify the latter failed due to its extreme air sensitivity. Therefore, in our last communication of this work,[2] compound 2^{2-} remained uncharacterized (and was there labelled 1^-). This complex has now been isolated in a much less air-sensitive form by exchanging the Na^+ cations with bis(triphenylphosphoranylidene)ammonium, $[N(PPh_3)_2]^+$. This large organic cation has been shown to stabilize other organometallic anions.[6] Crystallization of the $[N(PPh_3)_2]^+$ salt from thf with hexane, followed by recrystallization from CH_2Cl_2 and hexane, yields orange needles which are stable under nitrogen and for brief periods in air.

The IR spectrum of the sodium salt as formed in thf showed two carbonyl stretching bands at 1758 and 1872 cm^{-1}. Upon exchanging the cation, the $[N(PPh_3)_2]^+$ salt displayed carbonyl stretching bands in CH_2Cl_2 at 1788 and 1858 cm^{-1} (this salt could not be redissolved in thf for direct comparison). The difference in stretching frequencies, also observed for the NBu_4^+ salt in thf,[2] most likely arises from contact ion pairing with the Na^+ cations.

The ^1H NMR spectrum of complex 2^{2-} was far more complicated than might be expected. The reported spectrum[3d] for the *endo-endo* isomer of $[\{Mo(CO)_3\}_2(\eta^6:\eta'^6\text{-}C_{14}H_{14})]$, analogous to 2^{2-} in the solid state (see below), displays only four multiplets. The spectra of both the sodium salt prepared in $[^2H_8]$tetrahydrofuran and $[N(PPh_3)_2]^+$ salt dissolved in CD_2Cl_2 displayed 13 resonances, of which some were obviously overlapping multiplets. In addition, the ratios of the peak heights of some of the multiplets varied between the two salts. Variable-temperature studies from −60 (in CD_2Cl_2) to +80 °C (in $[^2H_6]$dimethyl sulfoxide, at which temperature decomposition occurred) failed to simplify the spectrum. However, a proton–proton correlated (90° COSY) two-dimensional NMR spectrum allowed us to group the resonances into three intracoupled sets (16 resonances total), which were assigned to the three possible isomers: *endo-endo*; *endo-exo*; and *exo-exo* (based upon the orientation of the protons attached to the bridging carbons of the bitropyl ligand).[3d] All three isomers were observed even when crystals representative of those on which X-ray crystallography was performed were examined. Since the crystal structure shows that 2^{2-} exists as the *endo-endo* isomer in the solid state, we infer that equilibration among the three isomers occurs upon dissolution of solid samples.

The ^1H–^1H coupling patterns of each cycloheptatrienyl ring depend upon whether the bridge proton is oriented *endo* or *exo*. In *endo* rings the H(1,7) protons couple separately with the H(2,6) protons as a chemically equivalent but magnetically inequivalent pair, and so there are two H(1,7)/H(2,6) coupling constants. The H(1) and H(7) protons also couple individually with H(3) and H(5), respectively, causing the H(1,7) protons to appear as a doublet of doublets of doublets. The H(2,6) protons couple only with H(1,7) and so appear as a doublet of doublets. The H(3,5) protons display one coupling constant to H(4), even when there are two chemically equivalent but magnetically inequivalent H(4) protons, as in the *endo-endo* and *exo-exo* isomers. Combined with the coupling to H(1) and H(7), this causes the H(3,5) protons to appear as doublets of doublets. The H(4) protons in both the *endo-endo* and *exo-exo* isomers couple differently to the H(3,5) protons on the attached ring and the adjoining ring, causing them to appear as triplets of triplets.

The ^1H NMR behaviour of the *exo* ring protons is somewhat different from that of the *endo* ring protons. All of the resonances except those of the H(4) protons show significant broadening, with the degree of broadening increasing with distance from the bridging carbons. The H(1,7) protons appear as very broad unresolved multiplets. The H(2,6) protons give overlapping doublets of doublets which appear as broadened triplets. The coupling constant between the H(1,7) and H(2,6) protons is apparently about half that between the H(2,6) and H(3,5) protons. The protons simply couple in order around the ring, H(1,7) to H(2,6) to H(3,5) to H(4), which in the absence of broadening would produce doublets of doublets for each proton except H(4). The H(4) protons in the *exo-exo* isomer give triplets of triplets as discussed above, but the H(4) protons in the *endo-exo* isomer give doublets of triplets, with coupling to each other and the H(3,5) protons on the same ring. No significant coupling between the H(4) and the H(3,5) protons on the adjoining ring could be observed for the *endo-exo* isomer.

The ^1H NMR data for the sodium salt are summarized in Table 1. Coupling constants and patterns were confirmed by selective decoupling experiments. An attempt more accurately to determine coupling constants and patterns by examining the ^1H NMR spectrum at 500 MHz yielded no additional information. As most of the ^1H NMR peaks were either closely spaced or actually overlapping at both 360 and 500 MHz, accurate integrals could not be obtained. However, comparison of the integrals of the relatively isolated peaks for the H(2,6) protons allowed an estimation of the isomer ratio of 2:3:1 for *endo-*

Table 1 Proton NMR spectral data for $Na_2[\{Mo(C_6F_5)(CO)_2\}_2(\eta^6:\eta'^6\text{-}C_{14}H_{14})]$ in $[^2H_8]$thf*

Isomer	H(1,7)	H(2,6)	H(3,5)	$H(4)_{exo}$	$H(4)_{endo}$
endo-endo	4.94, ddd (9.3, 5.1, 2.8)	4.74, dd (5.1, 2.8)	3.43, dd (9.3, 7.4)		0.78, tt (5.0, 2.3)
endo-exo	5.05, ddd (9.1, 5.0, 2.7)	4.90, dd (5.0, 2.7)	3.47, dd (9.1, 7.9)		0.85, dt (10.7, 7.9)
	5.50, m (br)	3.88, dd (8.6, 6.3)	3.26, dd (8.6, 7.7)	1.48, dt (10.7, 7.7)	
exo-exo	5.66, m (br)	3.98, dd (9.0, 4.5)	3.29, dd (9.0, 7.5)	1.55, tt (4.9, 2.2)	

* Chemical shift δ *vs.* $SiMe_4$. See Fig. 2(*b*) for numbering scheme. m = Multiplet, d = doublet, t = triplet, br = broad. Coupling constants in Hz in parentheses.

endo:*endo-exo*:*exo-exo* for the sodium salt in thf and 3:2:1 for the $[N(PPh_3)_2]^+$ salt in CD_2Cl_2.

The $^{13}C-\{^1H\}$ NMR spectrum of the sodium salt in $[^2H_8]$tetrahydrofuran displayed six resonances for co-ordinated ring carbons and four resonances for bridging carbons. Two-dimensional $^1H-^{13}C$ heteronuclear correlation (HETCOR) NMR spectroscopy was used to assign the carbon signals to the appropriate isomers and as an aid in assigning the ^1H signals. Surprisingly, it was found that, other than the bridging carbons, only the *endo* ring carbons were observable in the ^{13}C NMR spectrum. The broadened *exo*-^1H signals in the ^1H NMR spectrum showed no correlated ^{13}C signals. The lack of ^{13}C NMR signals for the *exo* ring carbons most likely resulted from their being broadened by the same process affecting the ^1H NMR signals. This broadening of the ^1H and ^{13}C signals of the *exo* ring may reflect a fluxional behaviour which is faster for the *exo* rings and becomes even faster farther away from the C(4)–C(4a) bridge. The reason(s) for this behaviour is not readily apparent to us. By contrast, each of the four types of bridging carbon, *endo* bound to *endo*, *endo* bound to *exo*, *exo* bound to *endo*, and *exo* bound to *exo*, has a unique ^{13}C resonance which could be correlated to the corresponding ^1H NMR resonance. The ^{13}C resonances for the phenyl and carbonyl carbons were observed at approximately δ 135–150 and 230–240, respectively, but could not be accurately assigned because of poor signal-to-noise ratios. The ^{13}C NMR data are summarized in Table 2.

Table 2 Carbon-13 NMR spectral data for the sodium salt in $[^2H_8]$thf[a]

Isomer	C(1,7)	C(2,6)	C(3,5)	$C(4)_{exo}$	$C(4)_{endo}$
endo-endo	105.4	82.1	73.7		50.2
endo-exo	105.3	82.4	72.9		49.7
	b	*b*	*b*	52.1	
exo-exo	*b*	*b*	*b*	51.6	

[a] Chemical shift δ *vs.* $SiMe_4$. See Fig. 2(*b*) for numbering scheme. [b] Not observed.

Cyclic voltammetry of the $[N(PPh_3)_2]^+$ salt in CH_2Cl_2 displayed an anodic peak at −0.85 V *vs.* ferrocenium–ferrocene coupled to a cathodic peak at −2.00 V, essentially identical to that of the NBu_4^+ salt generated by controlled-potential electrolysis of **1** in thf [Fig. 1(*b*)]. Controlled-potential electrolysis of the $[N(PPh_3)_2]^+$ salt at 0 V required 1.8 F per mol and produced a green solution, the cyclic voltammogram of which matched that of **1** [Fig. 1(*a*)].

Structure of $[N(PPh_3)_2]_2[endo\text{-}endo\text{-}\{Mo(C_6F_5)(CO)_2\}_2(\eta^6:\eta'^6\text{-}C_{14}H_{14})]\cdot thf$.—Selected internuclear distances and angles with estimated standard deviations for the $[N(PPh_3)_2]^+$ salt are listed in Table 3 and the structure of half of the molecule is shown in Fig. 2. The complex contains one solvent molecule of tetrahydrofuran (thf) in the unit cell which is disordered in two mutually incompatible sites adjacent to an inversion centre. The two halves of the bitropyl complex $[endo\text{-}endo\text{-}\{Mo(C_6F_5)(CO)_2\}_2(\eta^6:\eta'^6\text{-}C_{14}H_{14})]^{2-}$ are symmetry related about a centre of inversion at the midpoint of the bond joining the two cycloheptatrienyl rings. The central molybdenum atom is ligated by two terminally bound CO groups, a pentafluorophenyl group, and a cycloheptatrienyl ligand. The distance between the molybdenum atoms and the centroids of the tropyl rings is 1.743 Å. The experimental bond lengths between the molybdenum atoms and the carbonyl and pentafluorophenyl groups show no unusual deviation from expected values, see Table 3. The bond lengths and angles associated with the pentafluorophenyl, tetrahydrofuran and phenyl rings are also internally consistent and well within the range of published experimental values found in the Cambridge Structure Database.[7] The carbon–carbon distances observed in the cycloheptatrienyl groups are comparable to those found in the crystal structure of the complex $[\{Mo(CO)_3\}_2(\eta^6:\eta'^6\text{-}C_{14}H_{14})]$ by Adams *et al.*[3d]

The planarities of the six phenyl groups, the pentafluorophenyl ligand, and the cycloheptatrienyl ring have been tested. The least-squares planes program used in this structural analysis

Table 3 Selected internuclear distances (Å) and angles (°) for the complex $[N(PPh_3)_2]_2[endo\text{-}endo\text{-}\{Mo(C_6F_5)(CO)_2\}_2(\eta^6:\eta'^6\text{-}C_{14}H_{14})]\cdot thf$ with e.s.d.s in parentheses

Mo–C(8)	1.933(8)	Mo–C(9)	1.933(8)	Mo–C(1)	2.281(8)	Mo–C(2)	2.334(8)
Mo–C(3)	2.417(7)	Mo–C(5)	2.430(8)	Mo–C(6)	2.366(9)	Mo–C(7)	2.313(9)
Mo–C(11)	2.242(7)	C(8)–O(8)	1.173(9)	C(9)–O(9)	1.159(11)	C(1)–C(2)	1.359(13)
C(1)–C(7)	1.394(14)	C(2)–C(3)	1.387(10)	C(3)–C(4)	1.531(11)	C(4)–C(5)	1.548(11)
C(4)–C(4a)*	1.522(15)	C(5)–C(6)	1.379(10)	C(6)–C(7)	1.458(10)	C(11)–C(12)	1.370(9)
C(11)–C(16)	1.384(12)	C(12)–C(13)	1.367(11)	C(12)–F(12)	1.372(11)	C(13)–C(14)	1.366(14)
C(13)–F(13)	1.390(11)	C(14)–C(15)	1.371(11)	C(14)–F(14)	1.325(9)	C(15)–C(16)	1.353(11)
C(15)–F(15)	1.340(12)	C(16)–F(16)	1.394(9)	N–P(1)	1.585(6)	N–P(2)	1.574(7)
P(1)–C(21)	1.801(7)	P(1)–C(31)	1.790(7)	P(1)–C(41)	1.788(9)	P(2)–C(51)	1.786(7)
P(2)–C(61)	1.784(8)	P(2)–C(71)	1.805(7)	O(91)–C(92)	1.461(14)	O(91)–C(93)	1.419(14)
C(92)–C(95)	1.428(17)	C(93)–C(94)	1.436(17)	C(94)–C(95)	1.415(18)	Mo···centroid	1.743
C(8)–Mo–C(9)	79.8(4)	C(8)–Mo–C(11)	90.4(3)	C(9)–Mo–C(11)	90.5(3)	N–P(2)–C(61)	110.7(3)
Mo–C(8)–O(8)	177.2(8)	Mo–C(9)–O(9)	176.9(7)	Mo–C(11)–C(12)	124.3(6)	P(2)–C(61)–C(62)	122.0(6)
Mo–C(11)–C(16)	124.0(5)	C(3)–C(4)–C(4a)*	111.7(7)	C(5)–C(4)–C(4a)*	111.2(9)	N–P(2)–C(71)	109.6(4)
C(3)–C(4)–C(5)	109.5(6)	C(1)–C(2)–C(3)	128.7(9)	C(2)–C(3)–C(4)	126.7(8)	P(2)–C(71)–C(72)	118.4(5)
C(4)–C(5)–C(6)	127.4(6)	C(5)–C(6)–C(7)	127.3(8)	C(1)–C(7)–C(6)	126.4(8)	N–P(2)–C(51)	114.2(3)
C(7)–C(1)–C(2)	130.9(7)	P(1)–N–P(2)	140.4(4)	N–P(1)–C(21)	114.9(4)	P(2)–C(51)–C(52)	119.4(6)
N–P(1)–C(31)	106.4(3)	N–P(1)–C(41)	112.1(3)	P(1)–C(21)–C(22)	120.7(6)	C(92)–O(91)–C(93)	102.2(9)
P(1)–C(31)–C(32)	120.3(6)	P(1)–C(41)–C(42)	121.2(6)				

	Distance		Angle	
Ring	Mean	Range	Mean	Range
C(21)–C(26)	1.39(2)	1.36–1.41	120.0(5)	117.7–121.3
C(31)–C(36)	1.38(1)	1.36–1.39	120.0(14)	117.9–121.5
C(41)–C(46)	1.39(1)	1.37–1.41	120.0(5)	119.2–120.9
C(51)–C(56)	1.38(1)	1.37–1.40	120.0(8)	118.6–120.8
C(61)–C(66)	1.38(2)	1.36–1.41	120.0(13)	118.7–122.3
C(71)–C(76)	1.38(2)	1.36–1.41	120.0(11)	118.3–122.0

* Atom C(4a) is symmetry related to C(4) through a centre of inversion.

(*a*)

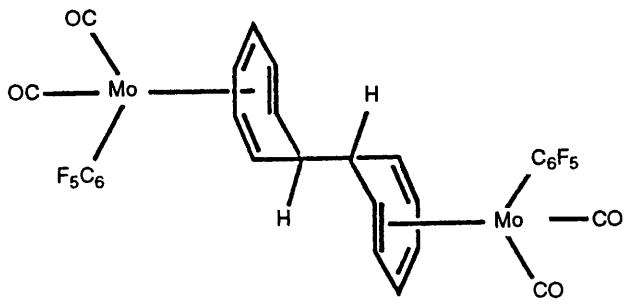

(*b*)

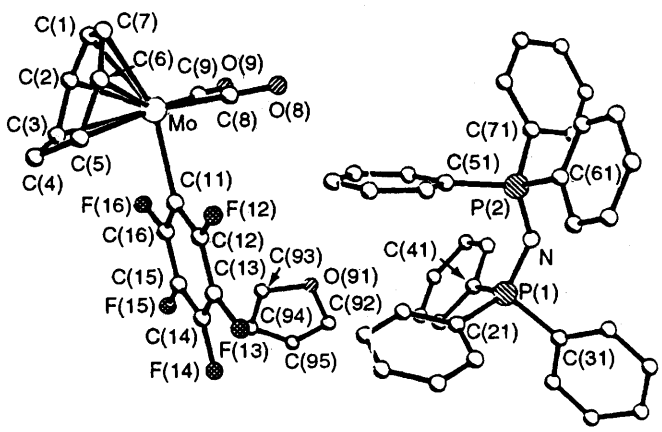

Fig. 2 (*a*) The dimeric scheme of the [*endo-endo*-{$Mo(C_6F_5)(CO)_2$}$_2$-(η^6:η'^6-$C_{14}H_{14}$)]$^{2-}$ anion. (*b*) Molecular structure of $[N(PPh_3)_2]_2$-[*endo-endo*-{$Mo(C_6F_5)(CO)_2$}$_2$(η^6:η'^6-$C_{14}H_{14}$)]·thf showing the atom labelling scheme

adapts the method developed by Schomaker *et al.*[8] The carbon atoms in the C_6F_5 ligand are planar with an absolute mean standard deviation of 0.006 Å. The largest deviation of the bonded fluorine atoms from the mean plane is 0.028 Å (range 0.003–0.028 Å). All the atoms within each tested phenyl ring also exhibit good planarity, as expected. Six carbon atoms of the cycloheptatrienyl fragment show good coplanarity (mean standard deviation 0.006 Å) and the envelope dihedral angle between this plane and that of the plane formed by the carbon atoms C(3)–C(5) is 136.4°. A packing diagram of the unit cell is shown in Fig. 3.

Experimental

General.—The complex $[Mo(C_6F_5)(CO)_2(\eta\text{-}C_7H_7)]$ **1** was prepared according to the literature procedure.[9] Solvents were distilled under nitrogen before use: CH_2Cl_2 (Fisher Optima) from CaH_2 and tetrahydrofuran (Fisher Optima) from sodium–benzophenone. All other chemicals were reagent grade or better. All reactions were carried out under an atmosphere of nitrogen or argon. Elemental analyses were performed by Texas Analytical Laboratories, Stafford, TX.

Instruments.—Infrared spectra were obtained using a Mattson Instruments Cygnus 100 FTIR, ^1H and ^{13}C-{^1H} NMR spectra on a Bruker AMX 360 NMR spectrometer. Chemical shifts were assigned relative to $SiMe_4$ as internal standard. Cyclic voltammetry and controlled-potential electrolyses were performed using a Bioanalytical Systems BAS

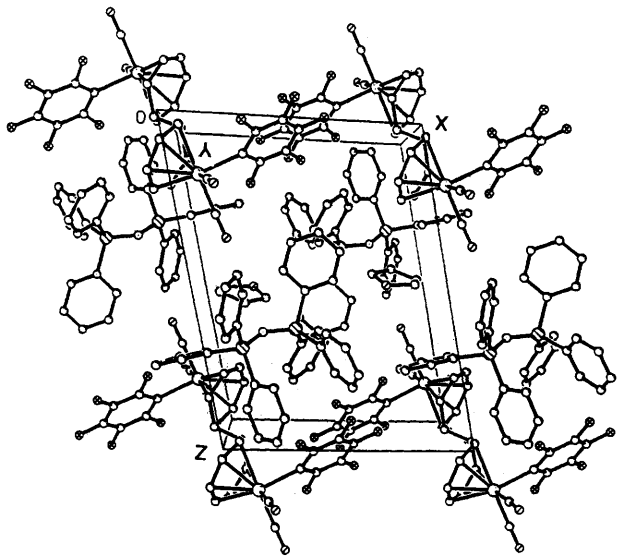

Fig. 3 Packing diagram for $[N(PPh_3)_2]_2$[*endo, endo*-{$Mo(C_6F_5)$-$(CO)_2$}(η^6,η'^6-$C_{14}H_{14}$)]·thf

100A electrochemical analyser. Conventional cyclic voltammetry was done using a 0.5 mm platinum disc working electrode, platinum-wire auxiliary electrode, and Ag–AgCl reference electrode. Fast-scan cyclic voltammetry used a BAS low-current module and a 10 μm platinum-disc working electrode. Controlled-potential electrolyses were performed using 25 × 25 mm platinum-foil working and auxiliary electrodes and a silver-wire quasi-reference electrode. All potentials are expressed relative to the formal potential of the ferrocenium–ferrocene couple, which we measure as approximately +0.45 V *vs.* Ag–AgCl.

Synthesis of $[N(PPh_3)_2]_2$[*endo-endo*-{$Mo(C_6F_5)(CO)_2$}$_2$-(η^6:η'^6-$C_{14}H_{14}$)]·thf.—Complex **1** (0.10 g, 0.24 mmol) was dissolved in tetrahydrofuran (3 cm^3), and 0.1% Na(Hg) (11.5 g, 0.50 mmol) was added. After stirring for 5 min, $[N(PPh_3)_2]Cl$ (0.14 g, 0.24 mmol) was added. The resulting precipitate of NaCl was filtered off to give an orange solution of the required $[N(PPh_3)_2]^+$ salt. The salt was precipitated by layering its thf solution with hexane, filtered off, washed with hexane, and then dissolved in CH_2Cl_2 (5 cm^3). Layering this solution with hexane yielded needle-like crystals (0.18 g, 76%) (Found: C, 64.8; H, 4.6; N, 1.3. $C_{106}H_{82}F_{10}Mo_2N_2O_5P_4$ requires C, 64.6; H, 4.2; N, 1.4%); ν_{max}/cm^{-1} (CO) 1859s, 1768s (CH_2Cl_2); δ_H(360 MHz, solvent CD_2Cl_2) 7.65 (m, Ph), 7.50 (m, Ph), 5.65 [m, $H(1,7)_{exo\text{-}exo}$], 5.50 [m, $H(1,7)_{endo\text{-}exo}$], 5.04 [ddd, $H(1,7)_{endo\text{-}exo}$], 4.94 [ddd, $H(1,7)_{endo\text{-}endo}$]. 4.93 [dd, $H(2,6)_{endo\text{-}exo}$], 4.77 [dd, $H(2,6)_{endo\text{-}endo}$], 3.96 [dd, $H(2,6)_{exo\text{-}exo}$], 3.86 [dd, $H(2,6)_{endo\text{-}exo}$], 3.46 [dd, $H(3,5)_{endo\text{-}exo}$], 3.40 [dd, $H(3,5)_{endo\text{-}endo}$], 3.27 [dd, $H(3,5)_{exo\text{-}exo}$], 3.24 [dd, $H(3,5)_{endo\text{-}exo}$], 1.53 [tt, $H(4)_{exo\text{-}exo}$], 1.48 [dt, $H(4)_{endo\text{-}exo}$], 0.78 [dt, $H(4)_{endo\text{-}exo}$] and 0.72 [tt, $H(4)_{endo\text{-}endo}$].

X-Ray Structural Analysis of $[N(PPh_3)_2]_2$[*endo-endo*-{Mo-$(C_6F_5)(CO)_2$}$_2$(η^6:η'^6-$C_{14}H_{14}$)]·thf.—*Crystal data.* $C_{106}H_{82}$-$F_{10}Mo_2N_2O_5P_4$, M_r = 1969.5, triclinic, space group, $P\bar{1}$ (no. 2, C_i^1), a = 11.862(2), b = 14.192(4), c = 15.189(1) Å, α = 77.20(1), β = 75.03(1), γ = 77.15(2)°, U = 2371.5(8) $Å^3$ (by least-squares fit of 25 well centred high-angle reflections), T = 292 K, Mo-K$\bar{\alpha}$ (λ = 0.710 73 Å), D_c = 1.379 Mg m^{-3}, Z = 1, $F(000)$ = 1006, μ = 0.396 mm^{-1}.

Data collection and processing. Three clear red irregularly shaped crystals (of dimensions 0.21 × 0.38 × 0.47, 0.34 × 0.42 × 0.68 and 0.33 × 0.46 × 0.52 mm) were selected on the basis of optical homogeneity and were mounted in sealed capillaries under a dry nitrogen atmosphere due to air

Table 4 Atomic coordinates ($\times 10^4$) with e.s.d.s in parentheses

Atom	*x*	*y*	*z*	Atom	*x*	*y*	*z*
Mo	938(1)	2 975(1)	1 651(1)	C(34)	12 236(8)	−3 130(7)	2 388(7)
C(8)	1 328(6)	1 558(6)	1 836(5)	C(35)	12 105(8)	−2 133(7)	2 408(7)
O(8)	1 565(5)	699(4)	1 986(5)	C(36)	11 012(7)	−1 586(6)	2 643(6)
C(9)	1 332(7)	2 706(6)	2 851(5)	C(41)	8 565(6)	−416(5)	3 794(5)
O(9)	1 582(6)	2 500(5)	3 567(4)	C(42)	9 045(6)	448(5)	3 432(5)
C(1)	−966(7)	3 729(6)	2 132(6)	C(43)	9 088(7)	1 052(6)	4 028(5)
C(2)	−304(7)	4 444(6)	1 958(5)	C(44)	8 662(7)	803(6)	4 962(4)
C(3)	514(7)	4 732(6)	1 161(5)	C(45)	8 177(7)	−40(6)	5 326(6)
C(4)	517(7)	4 652(5)	172(5)	C(46)	8 130(6)	−663(6)	4 742(5)
C(5)	503(6)	3 576(5)	127(5)	P(2)	6 316(2)	−2 048(1)	3 673(1)
C(6)	−310(6)	2 999(5)	655(5)	C(51)	5 439(6)	−954(5)	3 196(5)
C(7)	−1 012(7)	3 073(6)	1 586(6)	C(52)	5 145(6)	−143(5)	3 631(5)
C(11)	2 829(6)	3 081(5)	954(4)	C(53)	4 513(7)	722(6)	3 260(5)
C(12)	3 508(6)	2 534(5)	305(4)	C(54)	4 190(7)	787(7)	2 438(5)
C(13)	4 672(7)	2 578(6)	−96(5)	C(55)	4 483(7)	−2(7)	1 992(6)
C(14)	5 250(7)	3 205(6)	111(5)	C(56)	5 078(7)	−874(6)	2 370(5)
C(15)	4 611(7)	3 764(5)	764(5)	C(61)	6 192(5)	−3 027(5)	3 161(4)
C(16)	3 462(7)	3 693(5)	1 145(5)	C(62)	5 368(8)	−3 628(6)	3 571(6)
F(12)	3 027(4)	1 891(3)	18(3)	C(63)	5 226(8)	−4 351(7)	3 153(6)
F(13)	5 283(5)	2 002(5)	−759(4)	C(64)	5 978(8)	−4 517(7)	2 326(6)
F(14)	6 372(5)	3 258(5)	−290(4)	C(65)	6 802(8)	−3 935(6)	1 912(6)
F(15)	5 143(5)	4 386(4)	993(4)	C(66)	6 944(6)	−3 192(6)	2 337(4)
F(16)	2 912(5)	4 291(3)	1 805(3)	C(71)	5 655(6)	−2 346(5)	4 889(5)
N	7 655(5)	−1 974(4)	3 547(4)	C(72)	6 383(7)	−2 909(5)	5 484(5)
P(1)	8 555(2)	−1 242(2)	3 063(1)	C(73)	5 863(6)	−3 218(6)	6 381(5)
C(21)	8 313(6)	−519(5)	1 972(4)	C(74)	4 663(6)	−2 980(6)	6 719(6)
C(22)	7 573(7)	389(6)	1 937(6)	C(75)	3 957(8)	−2 423(6)	6 146(4)
C(23)	7 359(8)	895(7)	1 070(6)	C(76)	4 447(6)	−2 090(5)	5 239(4)
C(24)	7 828(8)	485(7)	298(7)	O(91)*	7 792(8)	3 543(7)	4 885(8)
C(25)	8 552(8)	−420(6)	321(7)	C(92)*	9 029(8)	3 577(7)	4 837(10)
C(26)	8 801(7)	−913(6)	1 176(5)	C(93)*	7 343(8)	4 532(8)	4 540(10)
C(31)	9 997(6)	−1 984(5)	2 839(5)	C(94)*	8 227(10)	5 136(7)	4 372(11)
C(32)	10 115(7)	−2 964(6)	2 834(6)	C(95)*	9 225(11)	4 562(9)	4 696(12)
C(33)	11 232(8)	−3 534(7)	2 606(7)				

* Solvent molecule, refined at site multiplicity = 0.5.

sensitivity. A conoscopic examination of the compound, using crystal rotation between two crossed polarizers on a Zeiss Photomicroscope (II), verified the optical quality and birefringent biaxial nature of the system. An Enraf Nonius CAD-4F automated diffractometer, equipped with a dense graphite monochromator, was employed to collect the crystal data. The ω–2θ scan technique was used within the limits $3.0 < 2\theta < 40.0°$ (h 0–11, k −13 to 12, l −14 to 13) with a varied scan angle of 0.46–3.44° min^{-1} in ω (ω scan range 1.20° + 0.34 tanθ) using Mo-K$\bar{\alpha}$ radiation. Data were collected on each of the three crystals until the intensities of the monitored standard decayed to 75% of the initial intensity measurements. The three data sets were corrected for decay (maximum correction 1.2317) and Lorentz and polarization effects, and then merged based on the intensity ratios of 50 reflections.[10] An empirical absorption correction, based on a Fourier series with coefficients obtained by minimizing the sum of the squares of residuals to calculate the absorption coefficients,[11] was applied (mean transmission coefficient 0.987). Of the 4430 independent reflections, 3698 fitted $F_i > 4.0\sigma(F_i)$ and were used in the structure analysis. An $N(Z)$ analysis (cumulative probability distribution test) provided credence to a centrosymmetric symmetry choice.[12]

Structure analysis and refinement. The phase problem was solved by the heavy-atom Patterson method (location of the main fragment: Mo, C_7, C_6F_5) and the standard Fourier-difference mapping technique on a personal computer using the SHELXTL-PC[13] package of programs. All non-hydrogen atoms were refined anisotropically using the block full-matrix least-squares procedure. Hydrogen atoms were included at calculated positions (C–H 0.96 Å) and allowed to ride on their respective bonding atoms with fixed isotropic thermal parameters (80×10^{-3} Å^2). The final cycle of refinement which included a secondary extinction correction [$g = 7.0(2) \times 10^{-4}$ e^{-2}] yielded reliability factors of $R = \Sigma(||F_o| - |F_c||)/\Sigma|F_o| = 0.073$ and $R' = [\Sigma w(|F_o| - |F_c|)^2/\Sigma w|F_o|^2]^{\frac{1}{2}} = 0.081$ and a 'goodness-of-fit' value of $S = 1.20$. The quantity minimized was $\Sigma w(|F_o| - |F_c|)^2$ and the weighting function $w = [\sigma^2(F) + 0.0086F^2]^{-1}$. A final electron-density map displayed some density (1.53 e^- Å^{-3}) in the vicinity of the molybdenum atom which is considered quite normal when dealing with heavy-metal atoms. However, elsewhere only a random fluctuating background was observed. Atomic scattering factors and associated anomalous dispersion correction factors were taken from the usual source.[14] Final non-hydrogen atomic coordinates according to the numbering scheme found in Fig. 2, are presented in Table 4.

Additional material available from the Cambridge Crystallographic Data Centre comprises H-atom coordinates, thermal parameters and remaining bond distances and angles.

Acknowledgements

We thank The Robert A. Welch Foundation (Grant Nos. AA-0668 and AA-1083) and Baylor University, in part, for support of this research. We are deeply indebted to Drs. James Karban and Nicholas Carr for much assistance in obtaining and interpreting the NMR spectra. We also express our appreciation to Dr. Ben Shoulders of the University of Texas at Austin for obtaining a ^{1}H NMR spectrum of the sodium salt at 500 MHz.

References

1 S. L. Gipson and K. Kneten, *Inorg. Chim. Acta*, 1989, **157**, 143.
2 S. L. Gipson, D. F. Mullica, E. L. Sappenfield, M. L. Hander and D. H. Leschnitzer, *J. Chem. Soc., Dalton Trans.*, 1992, 521.
3 (*a*) J. D. Munro and P. L. Pauson, *J. Chem. Soc.*, 1961, 3484; (*b*) V. R. Panter and M. L. Ziegler, *Z. Anorg. Allg. Chem.*, 1974, **453**, 14; (*c*) B. Olgemoller and W. Beck, *Chem. Ber.*, 1981, **114**, 867; (*d*) H. Adams, N. A. Bailey, D. G. Willett and M. J. Winter, *J. Organomet. Chem.*, 1987, **333**, 61.
4 A. M. Romanin, A. Venzo and A. Ceccon, *J. Electroanal. Chem. Interfacial Electrochem.*, 1980, **112**, 147; A. M. Romanin and A. Ceccon, *J. Electroanal. Chem. Interfacial Electrochem.*, 1981, **130**, 245.
5 C. P. Andrieux, L. Nadjo and J. M. Savéant, *J. Electroanal. Interfacial Electrochem.*, 1973, **42**, 223.
6 M. Darensbourg, H. Barros and C. Borman, *J. Am. Chem. Soc.*, 1977, **99**, 1647.
7 A. G. Orpen, L. Brammer, H. H. Allen, O. Kennard, D. G. Watson and R. Taylor, *J. Chem. Soc., Dalton Trans.*, 1989, S1.
8 V. Schomaker, J. Waser, R. E. Marsh and G. Bergman, *Acta Crystallogr.*, 1959, **12**, 600.
9 M. D. Rausch, A. K. Ignatowicz, M. R. Churchill and T. A. O'Brien, *J. Am. Chem. Soc.*, 1968, **90**, 3242.
10 Structure Determination Package, Enraf-Nonius, Delft, 1983.
11 N. Walker and D. Stuart, *Acta Crystallogr., Sect. A*, 1983, **39**, 159.
12 E. R. Howells, D. C. Phillips and D. Rogers, *Acta Crystallogr.*, 1950, **3**, 210.
13 SHELXTL-PC, Siemens Analytical X-Ray Instruments, Madison, WI, 1989.
14 J. A. Ibers and W. C. Hamilton, *International Tables for X-Ray Crystallography*, Kynoch Press, Birmingham, 1974, vol. 4.

Received 24*th May* 1993; *Paper* 3/02981F